ELSEVIER

Thermochimica Acta 382 (2002) 129–142

thermochimica acta

www.elsevier.com/locate/tca

Binary and ternary phase diagrams of two enantiomers in solvent systems

Heike Lorenz*, Andreas Seidel-Morgenstern

Max-Planck-Institut für, Dynamik komplexer technischer Systeme, Sandtorstraße 1, D-39106 Magdeburg, Germany

Received 17 April 2001; accepted 15 June 2001

Abstract

The binary phase diagram of the mandelic acid enantiomers and the binary and ternary phase diagrams of the same enantiomer(s) and water are studied as a typical enantiomeric system. The results of the experimental work performed are presented in detail and discussed both with regard to the applicability of different methods for solubility measurement and their importance for crystallization based enantioseparation. It will be shown that, in addition to classical methods differential scanning calorimetry (DSC) can be applied successfully for solubility determination. From the obtained phase diagrams various possibilities of gaining pure mandelic acid enantiomers from aqueous solutions are derived. The particular role of the eutectic composition in the enantiomeric system is emphasized.

Keywords: Phase diagram; DSC; Solubility; Enantiomers; Mandelic acid

1. Introduction

The detailed knowledge of fundamental solid/liquid equilibrium (SLE) data expressed in phase diagrams is essential for designing and optimizing crystallization processes. On the basis of the appropriate phase diagram it can be decided, if (fractional) crystallization can be applied for the separation or purification of a certain product of interest. Further, suitable operating conditions of an appropriate crystallization process can be specified. This is important both for the production of large scale (bulk) chemicals and special chemicals produced only in ''small'' amounts. Since more than 50% of the pharmaceutical active substances are known to be chiral [1], processes for enantioseparation and for finally recovering the solid enantiomer from solution are of large interest.

Enantioseparation and racemate resolution are frequently performed by means of crystallization methods, as there are the manual sorting of the crystals (from conglomerates), resolution by entrainment (preferential crystallization), separation via diastereomeric salt formation and crystallization from optically active solvents [2–4]. Furthermore, fractional crystallization can be used to get pure enantiomers from asymmetric (enantiomerically enriched) mixtures. In general, a final crystallization step is usually necessary to gain the solid enantiomer from its more or less diluted solution, even if other methods (chromatography, asymmetric synthesis) have been applied for racemate resolution. Contrary to inorganic and organic bulk products, where thermodynamic data for construction of the required phase diagrams are mostly available, for enantiomeric systems there is usually a lack of corresponding data. For this reason, crystallization processes of chiral products are sometimes carried out without detailed data just on the basis of experience. The knowledge of

* Fax: +49-391-6117-562.
E-mail address: lorenz@mpi-magdeburg.mpg.de (H. Lorenz).

0040-6031/02/$ – see front matter
PII: S0040-6031(01)00746-8

SLE data would help to optimize the process itself and, hence to increase the productivity.

The essential phase diagrams which have to be known are the binary melting point phase diagram describing the melting behavior of the two enantiomers, and for crystallization from solution, the binary pure enantiomer/solvent or the ternary two enantiomer/solvent solubility phase diagrams, describing the solubility behavior of the enantiomeric system in presence of a solvent.

Binary melting point phase diagrams are usually determined by thermoanalytical methods [5–7]. Particularly, differential thermal analysis (DTA) and differential scanning calorimetry (DSC) have proved to be capable of determining phase transitions and hence, these techniques are widely applied as analytical tools for pharmaceutical development [8–11]. The determination of phase diagrams by means of DSC has been reported for many years confirming its applicability and efficiency. Some examples from literature including recently published articles with the focus on designing crystallization processes are given in [12–14]. Generally, mixtures of different composition of the two components are prepared and the DSC curves resulting from a nonisothermal experiment using a low linear heating rate are measured. The melting points of pure substances are determined from the extrapolated onset temperature (T_e) of the melting effect [5,15]. For mixtures the solidus and liquidus line in the phase diagram are mostly taken from the extrapolated onset temperature T_e of the eutectic effect and the peak (T_p) [4,12,13] or extrapolated offset temperature (T_f) [16] of the dissolution effect of the excess component in the eutectic melt. However, the interpretation of DSC curves with respect to phase diagrams is not trivial at all. A comprehensive review on binary phase diagrams of chiral systems considering also reversible transitions which may occur between condensed phases (e.g. polymorphism, reversible decomposition of the racemate) was published recently by Coquerel [17].

The liquidus curve in the binary phase diagram of a chiral system can generally be predicted using a classical thermodynamic expression of the van't Hoff type, the so-called Schröder–van Laar equation [4]:

$$\ln(x\gamma) = \frac{\Delta H_m}{R}\left(\frac{1}{T_m} - \frac{1}{T}\right) \quad (1)$$

with x the mole fraction of the enantiomer in excess ($0.5 \leq x \leq 1$ for conglomerates; $x_{eu} \leq x \leq 1$ for compound forming systems (x_{eu}—eutectic composition)), γ the activity coefficient of the enantiomer in the mixture, ΔH_m and T_m the melting enthalpy (J/mol) and melting temperature (K) of the pure enantiomer, T the temperature of the mixture and R is the universal gas constant (J/mol K).

For an ideal mixture the activity coefficient is unity and Eq. (1) reduces to

$$\ln x = \frac{\Delta H_m}{R}\left(\frac{1}{T_m} - \frac{1}{T}\right) \quad (2)$$

Eqs. (1) and (2) represent the Schröder–van Laar equation in its simplified form neglecting the heat capacity term, which was found to be negligible in the case of enantiomers [4]. In the case of (ideal) compound forming enantiomeric systems the racemate branch in the phase diagram ($0.5 \leq x \leq x_{eu}$) can be calculated according to the Prigogine–Defay equation [4,18]

$$\ln(4x(1-x)) = \frac{\Delta H_{m,rac}}{R}\left(\frac{1}{T_{m,rac}} - \frac{1}{T}\right) \quad (3)$$

which is formally comparable to Eq. (2) but takes the different stoichiometric conditions into account. Analogous to Eq. (1) x represents the mole fraction of one of the enantiomers; $T_{m,rac}$ and $\Delta H_{m,rac}$ being the melting temperature and melting enthalpy of the racemic compound.

Even more scarcely available than the melting point phase diagrams are solubility data for the enantiomeric systems in a suitable solvent leading to the ternary solubility phase diagram of the system (+)-enantiomer/(−)-enantiomer/solvent. The reason seems to be the significant time exposure necessary for classical solubility measurements and, in the case of value added products, the comparatively "large" sample amount required. For this reason, various efforts have been carried out to develop advanced experimental possibilities for solubility determination directed to decrease the sample amount and the time required for the experiments as well as to improve the accuracy of classical methods.

Capewell et al. [19] described a new "apparatus and procedure for the measurement of solubility of rapidly equilibrating solid–liquid systems to 90 °C", which delivers solubilities for inorganic salts in water with an outstanding precision of ±0.05% and a deviation from

the well-known tabled values of ±0.1%. With up to 56 samples per experimental run it enables a high sample throughput, which is favorably in routine measurements. Nevertheless, it does not overcome the relatively high sample volume required, which is up to 50 ml saturated solution per experiment.

To reduce the amount of substance needed for solubility determination thermoanalytical methods like DSC attain special interest. One of the main advantages of the DSC in pharmaceutical development is the small sample amount (some mg) required for measurements. Recently, Endoh and Suga [20] and Myerson et al. [21] presented first results of solubility determination by means of thermogravimetry (TG) and DSC, respectively. Endoh and Suga [20] proposed the measurement of the mass loss due to evaporation of the solvent from an unsaturated solution of known concentration during a typical heating experiment in a conventional TG-DTA apparatus. When the solution composition crosses the solubility curve a slight change in the vaporization rate is indicated in the DTG curve. This effect is used to estimate the present solution composition and the appropriate temperature, thus providing one point in the phase diagram. The results presented refer to the solubility of NaCl, KCl and Na_2SO_4 in water. Limitations of the proposed new method seem to be the characteristics of the thermobalance (accuracy, sensitivity, resolution) responsible for the mass measurement (complete sample mass about 5 mg) and the evaporation rate of the solvent, which must not be too high. Own research results [21] are concerned with applying a conventional DSC apparatus for solubility measurements. The heat consumption due to the dissolution process during a controlled heating experiment is recorded and used to obtain the appropriate equilibrium temperature. First results with various organic compounds in different (aqueous and nonaqueous) solvents indicate the applicability of the technique.

These methods are quite novel and still in the development stage. However, they are promising methods for determination of solubilities as data basis for optimized crystallization from solution and, in the case of enantiomers, for their successful separation and enrichment by crystallization methods.

On the background given, in the present article the binary melting point phase diagram of the mandelic acid enantiomers and the ternary solubility phase diagram of the enantiomeric mandelic acid/water system are exemplarily studied to derive, finally, possible ways for a crystallization based enantioseparation. The experimental work to be described includes (a) the determination of the binary melting point diagram (+)-mandelic acid/(−) mandelic acid by means of DSC, (b) detailed measurements of ternary solubility data using a classical isothermal method with phase separation and subsequent analysis and (c) the estimation of solubilities applying a DSC method. The results are compared to literature values and discussed with respect to the applicability of the DSC technique (potential, efficiency) for solubility measurements. Furthermore, classical thermodynamic expressions are applied to evaluate the measured data in the binary system (+)-/(−)-mandelic acid. The importance of phase diagrams for enantioselective crystallization purposes is demonstrated for the separation of mandelic acid enantiomers from solution by means of vaporization and cooling crystallization techniques. Furthermore, on the basis of the experimental study described an optimized approach for estimating the ternary solubility phase diagram for an arbitrary enantiomeric system is proposed.

2. Experimental

The experimental part involves the application of two different methods for determination of phase diagrams: DSC for binary phase diagrams as a polythermal technique and a classical isothermal method for solubility measurements in the whole ternary system. In the following the methods are described in detail. The mandelic acid enantiomers {(+)-(*S*)- and (−)-(*R*)-mandelic acid} and the racemic (rac) mandelic acid as supplied from Merck or Aldrich were of synthesis grade (>99% purity), the water used as solvent was deionized. To investigate the potential of the DSC method additionally an enantiomeric system of relevance for the pharmaceutical industry was studied (no structure is given here). The acetonitrile chosen as solvent was of HPLC grade.

2.1. Application of DSC for phase diagram studies

The thermoanalytical investigations have been carried out using a SETARAM TG-DSC 111 apparatus in

the DSC mode. The DSC 111 is a Calvet type heat flux calorimeter, where the sample and the reference crucible are completely surrounded by the heat flow measurement thermopiles avoiding any errors due to local temperature distributions and heat loss. The heat flux sensor is calibrated by the Joule effect method, temperature calibration is performed regularly using the melting temperatures of high pure indium, tin, lead and aluminium for high temperatures and water for low temperatures. The calibration involves heating rates between 0.05 and 10 K/min as they cover the most commonly used. In all experiments the calorimeter was flushed with pure helium (99.999%) at a flow rate of about 8 ml/min.

The melting point phase diagram of the enantiomeric mandelic acid system was determined by heating samples (8–20 mg) of the pure enantiomers or any mixtures of them at a heating rate of 0.5 K/min in closed aluminium crucibles and recording the resulting DSC curve. The mixtures were prepared by previously weighing and mixing bigger sample amounts than required and crushing them together in a mortar. The mg-sample to be measured is then taken from this mixture. It could be shown that an optimal mixing effect is obtained in this way. A previously melting and annealing phase as usually applied for sample homogenization could not be performed, because mandelic acid decomposes significantly and irreversibly during the melting process. For this reason each sample could only be measured once. To evaluate the influence of the decomposition on the data related to the melting behavior, exemplary thermogravimetric experiments were carried out. Therefore, the TG-DSC 111 coupling was applied to correlate the heat effect with a simultaneous mass loss measurement. The melting point of the pure substances is obtained from the extrapolated onset temperature (T_e); the solidus and liquidus temperature for the mixtures are taken from the T_e of the eutectic effect and the peak temperature (T_p) of the subsequent dissolution effect.

A particular advantage of the SETARAM DSC 111 device with regard to *solubility measurements* is the comparatively large sample amount usuable, which is up to 150 μl in closed stainless steel crucibles and 250 μl in aluminum ones. This is important, because the low heating rates required to achieve equilibrium measurements generally lead to poor signal-to-noise ratios, when the heat loss/consumption rate is low, as it is the case in nonisothermal dissolution experiments. The solubility determination by DSC is based on the heat effect caused by the dissolution process. A mixture of known composition with an excess of solute is subjected to a constant heating rate and the temperature, where the last particles are just dissolved, is taken as the corresponding saturation temperature.

To prepare a solution of defined composition the required amount of solute is weighed in the crucible and the solvent is added with the help of a micropipette. The stainless steel crucible used is then crimped with an aluminum o-ring. It is gas tight and allows to withstand pressures up to 100 bar at 300 °C. To avoid errors due to evaporation of the solvent the actual mass of the solvent present at the measurement is calculated by weighing the crucible after it is crimped and no further evaporation is possible. The gas tightness could be confirmed exemplary by weighing back the crucibles after measurement cycles have been completed. Further sample preparation involves a first fast heating above the expected dissolution temperature and a subsequent annealing for about 20 min. This previous dissolving step avoids disturbing effects due to the heterogeneous (particulate) nature of the sample like the initial particle size of the solute and its distribution in the solution. After observing the recrystallization process during controlled cooling, the solubility measurement is started. Full sample amounts were between 50 and 110 mg, the optimal heating rate was found to be 1 K/min. A more detailed description of the method applied will be published soon [22].

2.2. Solubility measurements and the determination of the ternary (solubility) phase diagram of the enantiomeric mandelic acid system

For determination of solubilities in the ternary system the well-known isothermal method with phase separation and subsequent analysis [23] (adapted to chiral systems) has been applied.

An excess of either pure enantiomer or a mixture of known enantiomeric composition was added to a certain amount of solvent in a closed glass container (volume 20 or 50 ml). This container was immersed in a double or triple walled thermostated equilibrium apparatus and the solution was then electromagnetically stirred at the desired temperature (temperature

controlled to within ±0.02 K) until equilibrium was achieved (at least 4 h). The time required for establishing the solid/liquid equilibrium was determined in a separate experiment, withdrawing and analyzing samples of the mother liquor after different time intervals during dissolution studies. It could be shown that, at 25 °C the equilibrium has already been attained after 20 min for both the (+)-mandelic acid enantiomer and the racemate. For ternary systems containing both mandelic acid enantiomers and water, the liquid and solid phase (saturated solution and undissolved solid) were analyzed to determine their composition. The amount of solute in the saturated solution was determined by evaporating the solvent in a rotary evaporator. Comparatively the mandelic acid concentration in the solution has also been estimated by alkalimetric titration against 0.1 m NaOH. The (+)- to (−)-enantiomer ratio (enantiomeric composition) was analyzed by HPLC. Finally, the quality of the results could be assessed from an overall mass balance. For binary systems consisting of a pure enantiomer and the solvent, only the liquid phase was examined taking a liquid sample with the help of a pipette after allowing the solid phase to settle and then evaporating the liquid sample. The sample amounts used for solubility measurements were always related to 5 or 10 ml of water as solvent. Additionally, experiments with ''small'' sample amounts related to 0.5, 1 and 2 ml water have been performed to evaluate the applicability of this classical method for solubility determination of value added pharmaceutical substances. Mixtures of different enantiomeric composition were always prepared by adding the appropriate amount of the excess enantiomer to racemic mandelic acid.

About 55 points in the ternary phase diagram (+)-mandelic acid/(−)-mandelic acid/water have been measured allowing to specify solubilities at temperatures between 0 and 60 °C covering the whole range of enantiomeric compositions.

3. Results and discussion

In the following the binary and ternary phase diagrams obtained for the enantiomeric mandelic acid system are presented and discussed. The two different methods applied for solubility determination are compared. Finally, on the basis of the ternary solubility phase diagram possibilities for enantioselective crystallization in the system studied are derived.

3.1. Binary melting point phase diagram of the mandelic acid enantiomers

In Fig. 1 DSC curves measured for mixtures of different enantiomeric composition between the

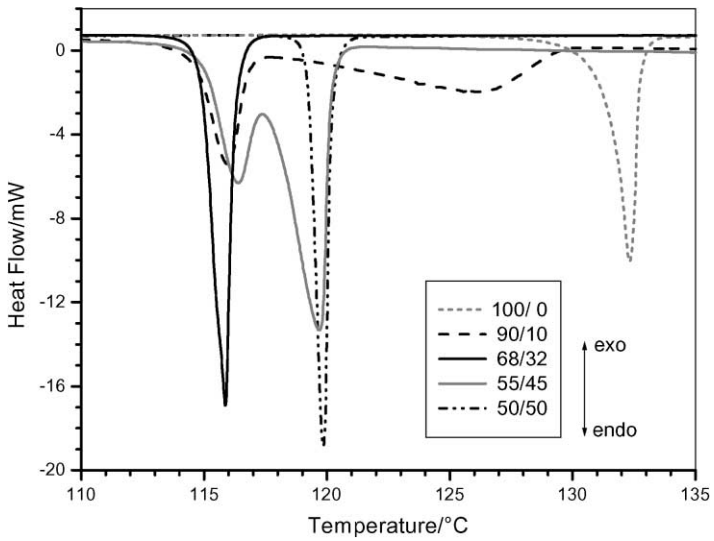

Fig. 1. DSC curves of different mixtures of mandelic acid enantiomers (100/0 corresponds to $x = 1$, 90/10 to $x = 0.9$, etc.).

racemic composition ($x = 0.5$) and the pure enantiomer ($x = 1$) are presented. Three sharp melting effects at 131.6 °C for the pure enantiomer, 120.2 °C for the racemic mixture and at 114.8 °C for a mixture containing the enantiomers in the ratio of 68.23:31.77 are obtained. The latter indicates the eutectic in the mandelic acid enantiomeric system. The racemic mixture shows a melting point between the eutectic and the pure enantiomer. Thus, at the racemic composition a real compound is formed in the solid state containing both enantiomers in equal quantities (racemic compound or ''true'' racemate). According to the classification of Roozeboom [24] the system under study can thus be assigned to the compound forming type with a melting point minimum for the racemate compared to the pure enantiomer. Mixtures between the eutectic composition and the pure enantiomer (e.g. sample 90/10 in Fig. 1) or the eutectic and the racemate (sample 55/45 in Fig. 1) show a melting region consisting of the eutectic effect and the subsequent dissolution effect, where the excess component (pure enantiomer or racemate, respectively) are dissolved in the liquid (melt) phase.

The resulting binary melting point phase diagram is presented in Fig. 2. As the two enantiomers of a chiral compound are characterized by the same melting point, a symmetric phase diagram around $x = 0.5$ is obtained. For this reason only one-half of the phase diagram ($0.5 \leq x \leq 1$) is shown in Fig. 2. The symmetry of the diagram could be confirmed by DSC experiments with both, mixtures containing the (+)- and the (−)-enantiomer in excess. As already indicated above, the phase diagram shows the typical form of a compound forming system with a racemic compound having a lower melting point than the pure enantiomer. The comparison with literature data reveals a good agreement with the pure substance data published recently by Li et al. [26], but a discrepancy to the results of Leclercq [25] and the very old detailed data given in [27]. However, the deviation obtained is mainly in the range of ±3 K, i.e. smaller than ±3% of the melting temperature. Even the melting point of the racemic mandelic acid and its (−)-enantiomer is given in the Ullmann Encyclopedia [28] to be between 118–121 and 132–135 °C, respectively. The melting enthalpies were determined from DSC measurements to be 24.5 kJ/mol for the pure enantiomers and 25.6 kJ/mol for the racemate. For comparison in the literature values of 26.4 and 25.1 kJ/mol [25] as well as 25.7 and 26.8 kJ/mol [26] are given. The eutectic was reported before to vary between $x = 0.6$ and 0.7 [27,29].

The main problem seems to be the significant decomposition of the mandelic acid during the melting process, making it principally impossible to identify a real ''melting point''. Furthermore, mandelic acid is known to be unstable when exposed to light [28,30]. Repeatability measurements with the pure enantiomers and the racemate have shown, that the error in the determination of the melting temperature and the

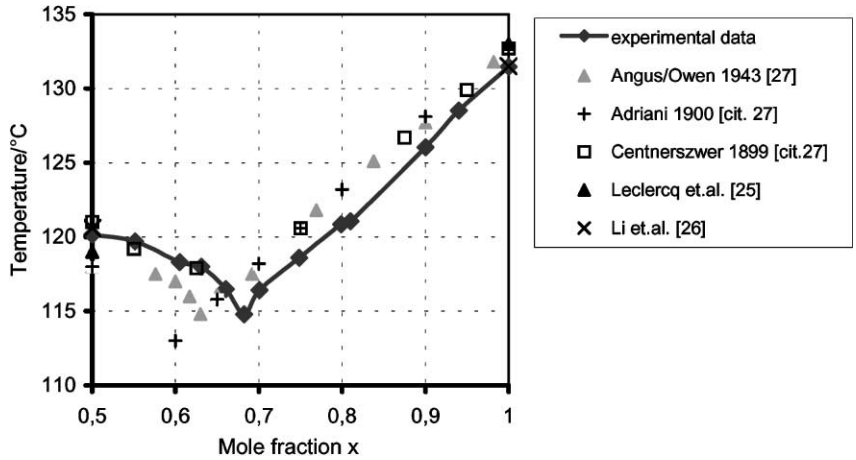

Fig. 2. Binary melting point phase diagram of the mandelic acid enantiomers.

melting enthalpy are below ±0.2 and ±1.4%, respectively. The mass loss due to decomposition was estimated by means of TG-DSC coupling to be 2.2 wt.% until the melting starts (T_e) and 2.8 wt.% at the end of the melting peak. Thus, this error should be kept in mind when evaluating the accuracy of the given melting temperatures and melting enthalpies.

When using the obtained pure component data (T_m, ΔH_m, $T_{m,rac}$, $\Delta H_{m,rac}$) for calculating the liquidus curves by means of the simplified Schröder–van Laar and Prigogine–Defay equations (Eqs. (2) and (3)) no satisfying agreement between the estimated and experimental curve was obtained. Around the eutectic (between about x = 0.6 and 0.8) the liquidus lines predicted showed a significant deviation to lower temperatures. As a result, the eutectic temperature was calculated to 112.2 °C compared to an experimental value of 114.8 °C. Although, generally ideal behavior of the liquid melt phase is assumed in a binary chiral system, sometimes nonideality is described in literature [31]. This is reported in cases, where the enantiomers tend to associate and the responsible groups in the molecule are located nearby the chiral center. In the binary system (+)-/(−)-mandelic acid association is likely to take place, caused by the presence and neighborhood of a hydroxyl and a carboxyl group in the mandelic acid molecule allowing both intramolecular and intermolecular interactions (hydrogen bond, dimerization, etc.). Fig. 3 shows the calculated liquidus lines in the phase diagram when fitting the experiments by means of Eqs. (2) and (3) using the most certain (accurate) data points near the pure component sides ($x \leq 0.605$; $x \geq 0.799$). As result, the eutectic composition could be specified to 0.69/0.31, corresponding well with the result (0.7) from Fouquey and Jacques [29]. The melting enthalpies were determined to be 31.2 kJ/mol for the racemate and 28.1 kJ/mol for the enantiomer, what is considerably higher than the experimental data and expected from the significant sample decomposition during melting.

3.2. Solubility phase diagrams of the pure mandelic acid enantiomers and the racemate

To determine the ternary solubility phase diagram of the mandelic acid enantiomers in water two experimental methods, a classical isothermal method in a solubility apparatus and a polythermal DSC based technique, have been applied. The results obtained are summarized in Figs. 4–8.

In Fig. 4 the solubility of the racemic mandelic acid and its (+)-enantiomer in water is presented as function of temperature. In both cases the solubility increases with temperature. The racemate is not only higher soluble than the pure enantiomer (as already derivable from the melting points), but also shows a different temperature dependency of the solubility.

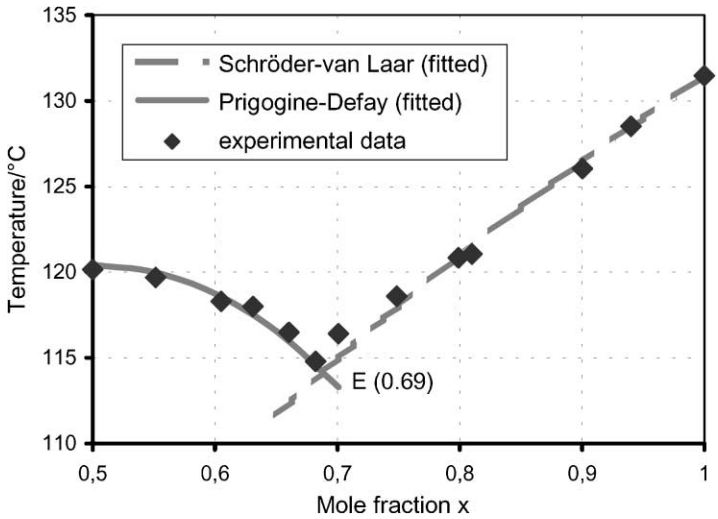

Fig. 3. Binary melting point phase diagram of the mandelic acid enantiomers—fitted and experimental values.

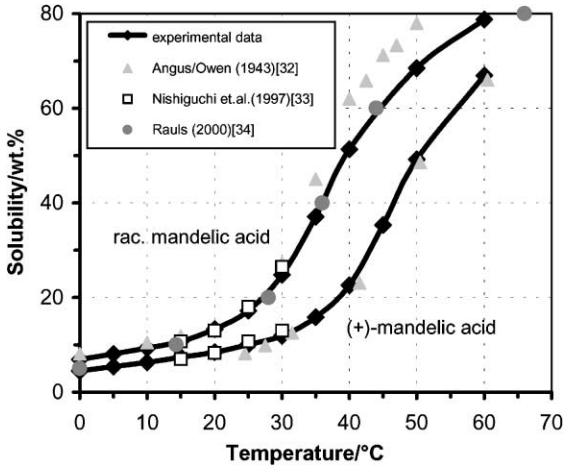

Fig. 4. Solubility of mandelic acid in water as function of temperature (classical isothermal method).

The rapid rise of the solubility following a rather moderate increase starts at a significantly lower temperature level (about 10 K) compared to the enantiomer. This leads to considerable differences in the solubilities of the racemate and the enantiomer at temperatures higher than 30 °C. There are regions, where the solubility of the racemate is twice as high as for the (+)-mandelic acid. The most favorable conditions, a cooling crystallization process for gaining the solid substance from the solution should be operated at, are given in the region with the strongest effect

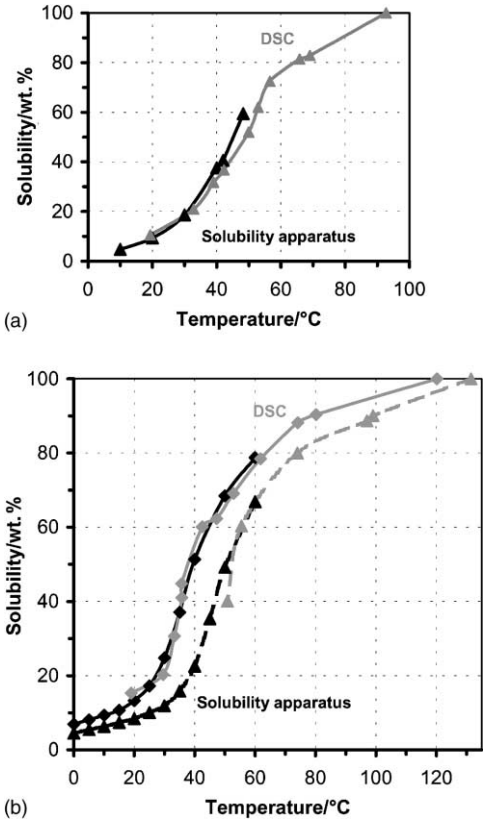

Fig. 6. Applicability of different methods for solubility measurement—solubility as function of temperature for (a) enantiomer A, (b) (◆) racemic mandelic acid, (▲) (+)-mandelic acid.

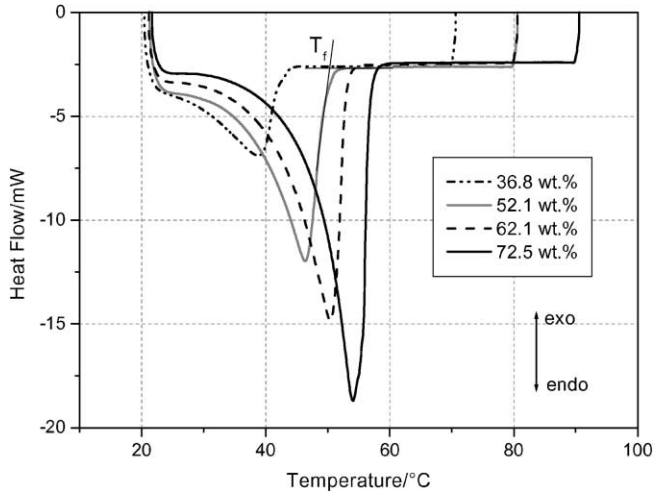

Fig. 5. Illustration of typical DSC curves for solutions of different concentration of enantiomer A in acetonitrile (heating rate: 1 K/min; total sample mass: 68–78 mg).

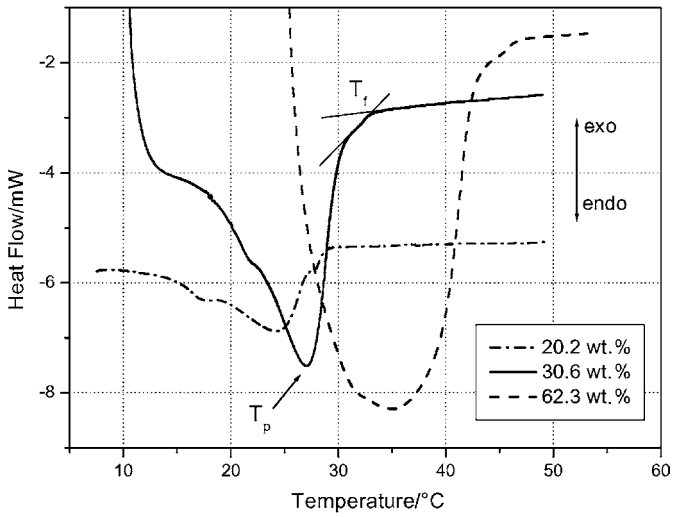

Fig. 7. DSC curves for solutions of racemic mandelic acid in water of different concentration (heating rate: 1 K/min; total sample mass: 79.034, 98.795, 97.527 mg).

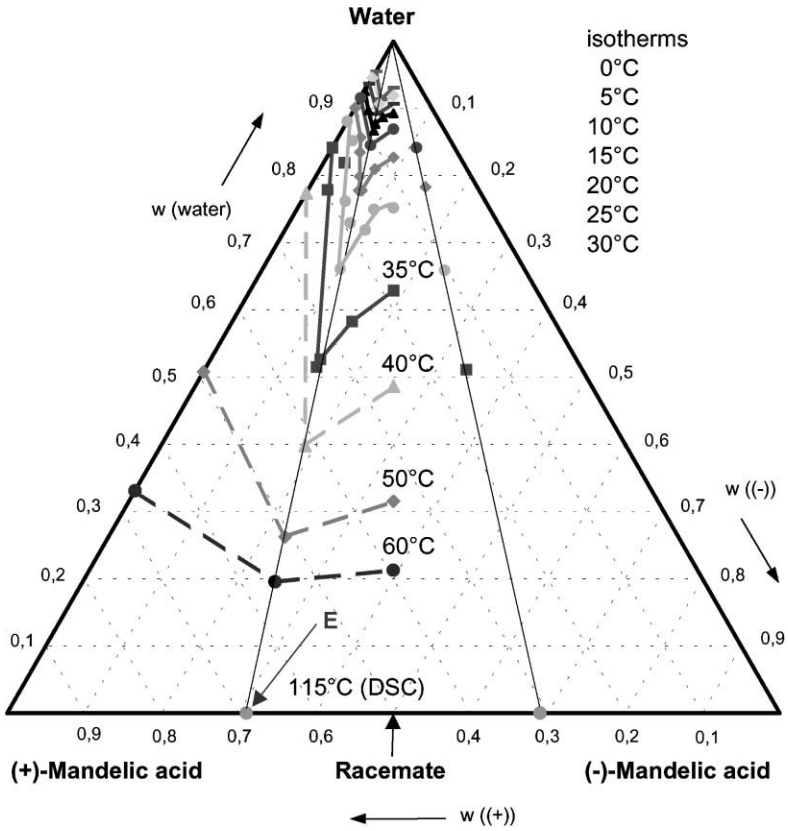

Fig. 8. Ternary (solubility) phase diagram of the enantiomeric mandelic acid/water system (graduated in weight fraction units (w)).

of temperature on solubility. This corresponds to the steepest slope in the solubility curve which is between about 30 and 40 °C for the racemate and 40 and 50 °C for the pure enantiomer. The solubility data measured are found to be in good agreement with the very few literature sources. However, the discrepancy to the high temperature racemate solubility data given by Angus and Owen [32] cannot conclusively be explained. The maximal error of the solubility data in the temperature range reported was estimated to be smaller than 2.5% by means of repeatability measurements. Higher errors are mostly caused by too low amounts of solvent and solute when phase separation becomes difficult. In our case it could be shown that at least 1 ml solvent and about 100 mg solute should be considered as the lower limits.

The results of solubility determination by means of the DSC method are presented in Figs. 5–7. Fig. 5 shows for illustration the DSC curves obtained for different mixtures of the pure enantiomer of the pharmaceutical relevant specialty chemical (enantiomer A) in acetonitrile. Broad endothermal effects are observed, caused by the continuous heat consuming dissolution process of the solid enantiomer in the solvent. From the increasing offset temperatures (T_f) obtained for higher solution concentrations a positive slope of the solubility curve is expected. Under equilibrium conditions the course of the dissolution effect in the DSC curve should follow the solubility curve. Then, the end of this effect (characterized typically by T_f) corresponds to the saturation temperature at the given solution composition. In the case of a nonequilibrium measurement (often typical in DSC experiments) the dissolution process is determined by kinetic effects (especially diffusion phenomena).

To validate the applicability of the DSC method, in Fig. 6 the saturation temperatures derived from the DSC curves are compared to solubility data determined by means of the applied classical method. This comparison is shown for the enantiomer A (Fig. 6a) as well as for mandelic acid (Fig. 6b). Obviously, the agreement of the results is satisfying.

However, whereas for the system enantiomer A–acetonitrile very distinct thermal effects were observed, for the mandelic acid–water system (particularly the (+)-mandelic acid) the information was less transparent. So, the DSC curves were not always that ''peak shaped'' and sharp at the end as demonstrated for the enantiomer A.

Characteristic DSC curves for different mixtures of racemic mandelic acid in water are presented in Fig. 7. The saturation temperatures were determined from the offset temperatures (T_f) as indicated. In the case of (+)-mandelic acid the dissolution effects observed were very flat and T_f could not exactly be identified. Thus, the saturation temperatures included in Fig. 6b were taken from the peak temperature (T_p), which was always clearly recognizable. The dissolution process of (+)-mandelic acid in water seems to be significantly influenced by kinetic effects under the applied DSC conditions.

The problem of performing equilibrium measurements under DSC conditions in heterogeneous solid–liquid systems, which are expected to be strongly influenced by diffusion effects, cannot be solved principally. A first complete dissolution and annealing step before carrying out the solubility measurement (as it has been done) helps to minimize the disturbing effects of the initial particle size and the initial unfavorable distribution of the solute in the DSC crucible, but does not compensate the missing stirring and, the required well mixed solution. Consequently, the DSC method is not able to replace common (classical) techniques for solubility measurements, but it can additionally be used when only very low sample amount is available and high temperature/pressure measurements are required. When using the applied classical method, in minimum some grams both of the racemate and the pure enantiomer are needed to determine the ternary solubility diagram (in the way it has been done) for a well soluble system with a strong effect of temperature on solubility. The polythermal DSC technique can at least be used to ''scan'' quite quickly the temperature dependency of the solubility in only one high temperature run and to get first rough solubility data.

However, more testing and a theoretical analysis of the method are required. Further details will soon be published [22].

3.3. Ternary solubility phase diagram of the mandelic acid enantiomers in water

In Fig. 8 the equilibrium data determined in the ternary system (+)-mandelic acid/(−)-mandelic

acid/water are summarized and presented in the typical equilateral triangle shaped diagram. There, the vertices represent the pure components involved, i.e. the two mandelic acid enantiomers on the triangle base and the water as solvent at the top. As follows, the triangle sides illustrate the binary systems (+)-mandelic acid/water and (−)-mandelic acid/water on the left- and right-hand sides and the (+)-/(−)-mandelic acid on the base. A further (quasi)binary system racemate/water is formed by the connection line between the racemic composition on the triangle base ($w = 0.5$) and the water corner. Each point inside the diagram represents a mixture consisting of all three components and hence, reflects the solubility of a mixture of given enantiomeric composition at the temperature applied. Thus, connecting all points belonging to the same temperature defines the solubility curve of the ternary system at this temperature. Above the particular saturation isotherm the solution is undersaturated, i.e. only one phase (a liquid) exists, below the isotherm two or three phases (a liquid and one or two solid phases) are formed.

Corresponding to the binary enantiomeric system, the solubility experiments concentrated primarily to mixtures with (+)-mandelic acid in excess; for mixtures containing the (−)-enantiomer in excess only a few measurements have been carried out to confirm the expected mirror image symmetry. So, the right-hand side of the ternary phase diagram may be constructed by reflecting the solubility curves in the triangle (+)-mandelic acid–racemate–water about the racemate–water line. The strong temperature dependency of the solubility for both the pure enantiomer and the racemate in a medium temperature range (as described already in Fig. 4) is represented in the ternary solubility diagram by increasing distances between the saturation isotherms. Starting on an isotherm from the pure mandelic acid enantiomer side and the racemate composition, the solubility grows steadily approaching a certain maximum, the appropriate eutectic point. As a result, the solubility curve gets the typical shape expected for a compound forming system. The eutectic was found to be independent on temperature at an enantiomeric composition of 69:31 (or vice versa) matching the eutectic in the binary mandelic acid system. This value is in agreement with the only literature source available [33]. The region in the phase diagram, where finally enantiomerically pure mandelic acid can be crystallized from its aqueous solution at a given temperature, is then determined by the triangle limited by the pure enantiomer corner, the pure enantiomer solubility and the solubility of the eutectic mixture (existence region of the enantiomer).

Possible procedures of performing enantioselective crystallization in the mandelic acid system will be demonstrated on the basis of the schematic illustrations of the ternary phase diagram shown in Fig. 9a for the case of a vaporization crystallization and in Fig. 9b for a cooling crystallization. Starting from a partially resolved solution of composition P (Fig. 9a),

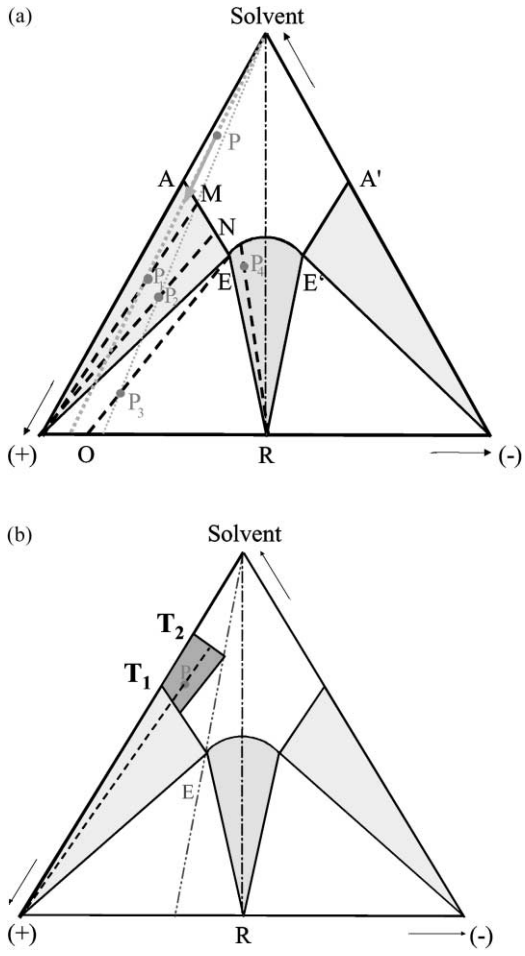

Fig. 9. Enantioselective crystallization from solution for a compound forming enantiomeric system. (a) Vaporization crystallization; (b) cooling crystallization.

vaporization of the solvent gives a solution of e.g. composition P_1, which splits into a solid phase consisting of the pure (+)-enantiomer and a saturated solution of composition M on the appropriate solubility curve. After separating the solid, solution M can repeatedly be evaporated reaching e.g. point P_2, delivering again crystals of the pure (+)-enantiomer and a saturated solution of composition N. Depending on the initial mixture and the procedures performed a few crystallization steps can be carried out ending up with a saturated solution of eutectic composition E. The amount of pure enantiomer to be gained by such a fractional crystallization process can be calculated directly from the phase diagram using the lever rule [36]. It should be noted that during these fractional crystallization steps the solution composition must not leave the existence region of the pure enantiomer. If, e.g. too much solvent has been evaporated, the solution composition enters the three-phase region defined by the triangle (+)-enantiomer–E–R, where the enantiomer and the racemate crystallize together and consequently, no pure (+)-enantiomer can be recovered anymore. Thus, a solution P_3 splits into a mixture of racemate and (+)-enantiomer of composition O and a saturated solution of eutectic composition. Furthermore, if the enantiomeric composition in the initial solution is lower than the eutectic, no further enantiomeric enrichment can be achieved. A solution composition inside the region E–R–E′ (e.g. P_4) always delivers the racemate as the stable solid phase.

In the case of a cooling crystallization (Fig. 9b), an initial solution of composition P, located outside the pure enantiomer existence region at a high temperature T_1, becomes supersaturated, when cooling to a lower temperature T_2. Resulting from this, the pure (+)-enantiomer crystallizes. Due to the strong temperature dependency of the mandelic acid solubility both vaporization and cooling crystallization techniques can be applied to gain the solid enantiomer from its aqueous solution.

3.4. Conclusions

On the basis of the binary and ternary phase diagrams the enantiomeric mandelic acid could be identified as a compound forming system. Thus, racemic mandelic acid forms a real 1:1 compound in the solid state. Consequently, the racemate cannot be resolved by crystallization methods without any auxiliary optically active agent (solvent or a resolving agent for diastereomer formation). Resolution by entrainment, also called preferential crystallization, is successfully applicable only in the case of conglomerate forming systems and, thus not suitable for the given system. However, fractional crystallization allows to gain pure enantiomers, if the initial solution composition is located in the existence region of the desired enantiomer in the appropriate phase diagram. Thus, for mandelic acid the pure (+)- or (-)-enantiomers can directly be crystallized from an aqueous solution or the melt, if their ratio is higher than 0.69:0.31, respectively.

For this reason a two-step process consisting of a previous racemate resolution step and a subsequent crystallization step for further purification offers the possibility of producing pure enantiomers. The first step could be a chromatographic or advanced membrane separation process, as they are already applied or under intensive research in the case of enantiomeric drugs. Replacing such comparatively expensive separation techniques partly by usually cheaper crystallization procedures should result (when optimized) in higher efficiencies and/or productivities for the whole combined process. Anyway, the fundamental solid/liquid phase equilibria and, particularly the position of the eutectic point, determine the transition region between the two steps for enantioseparation. In the case of mandelic acid the previously performed chromatography must deliver a minimum enantiomeric enrichment higher than 0.69:0.31. It could be shown in a previous study that, a purity requirement of 70% instead of >99% for the chromatographic step allows a productivity increase of about one order of magnitude [35].

The estimation of ternary solubility phase equilibria has proved to be a time and sample consuming process. Especially in the case of valuable pharmaceuticals like certain enantiomeric drugs the sample amounts required for systematic solubility studies may be a problem. However, to scan the possibilities for enantioseparation by means of different crystallization methods and to optimize them subsequently, reliable and accurate data are of essential importance. To reduce the time exposure and to minimize the amount of substance for the experiments to be

performed, the following approach is suggested as a result of the presented study.

1. ''Scanning'' the binary melting point phase diagram of the enantiomeric system to specify its type and the eutectic composition (DSC experiments using the enantiomer, the racemate and several mixtures of them; check for substance stability by repeated runs).
2. If the eutectic composition cannot be specified with sufficient accuracy by experimental work the prediction of the phase diagram by theory (using the reliable experimental data) may be helpful.
3. Determining the solubility of the pure enantiomer, the racemate and, in the case of true racemates, the eutectic mixture as function of temperature. In addition to the common classical methods usually applied, DSC can be recommended, when only small sample amount is available and high temperature/pressure data are required. When using a classical method to measure the solubilities of value added products, the amount of solute and solvent per sample should be optimized to save substance.
4. Construction of the ternary solubility phase diagram. The temperature dependency of the pure enantiomer existence region allows to choose a suitable crystallization technique.

4. Summary

In the contribution the binary and ternary phase diagrams of the mandelic acid enantiomers in water have been studied. From the melting point phase diagram the mandelic acid enantiomeric system could be identified as a compound forming system with a melting point of the racemate lower than for the enantiomers. This is in agreement with the racemate solubility, which was measured to be considerably higher compared to the enantiomers. Furthermore, the ternary solubility phase diagram revealed a strong temperature dependency of the solubility and an eutectic at an enantiomeric composition of 0.69:0.31. Thus, pure mandelic acid enantiomers can be gained from partially enriched solutions having an enantiomeric composition higher than this eutectic, whereby both cooling and evaporation crystallization techniques are applicable. It could be shown that, the exact knowledge of the eutectic composition is of particular importance for assessment of crystallization based enantioseparation. As racemic mandelic acid cannot be resolved by crystallization alone, a two-step procedure consisting of a previous chromatographic step resolving the racemate and delivering the required enantiomeric enrichment followed by a subsequent (fractional) crystallization step has been proposed. Moreover, it could be demonstrated that, additionally to common methods DSC can be applied for the determination for solubility data for value added (pharmaceutical) products.

Acknowledgements

The authors thank Jacqueline Kaufmann and Dragomir Sapoundjiev for help during the extensive experimental work and Fonds der Chemischen Industrie for financial support.

References

[1] H. Brunner, Rechts oder links: in der Natur und anderswo, Wiley, Weinheim, 1999.
[2] R.M. Secor, Chem. Rev. 63 (1963) 297.
[3] A. Collet, Enantiomer 4 (1999) 157.
[4] J. Jacques, A. Collet, S.H. Wilen, Enantiomers, Racemates and Resolutions, Krieger, Malabar, 1994.
[5] W.F. Hemminger, H.K. Cammenga, Methoden der Thermischen Analyse, Springer, Berlin, Heidelberg, 1989.
[6] M.E. Brown (Ed.), Principles and practice, in: Handbook of Thermal Analysis and Calorimetry, Vol. 1, Elsevier, Amsterdam, 1998.
[7] E.L. Charsley, S.B. Warrington (Eds.), Thermal Analysis: Techniques and Applications, Royal Society of Chemistry, Cambridge, 1992.
[8] D. Giron, Pharmaceutical Science and Technology Today (PSTT) 1 (1998) 191 and 262.
[9] D. Giron, J. Therm. Anal. Calorimet. 56 (1999) 1285.
[10] S.-D. Clas, C.R. Dalton, B.C. Hancock, PSTT 2 (1999) 311.
[11] K.C. Thompson, Thermochim. Acta 355 (2000) 83.
[12] M. Siniti, S. Jabrane, J.M. Letoffe, Thermochim. Acta 325 (1999) 171.
[13] M. Matsuoka, R. Ozawa, J. Crystal Growth 96 (1989) 596.
[14] H. Takiyama, Y. Nishitani, M. Matsuoka, Automatic determination of solid–liquid phase equilibria by using measured DSC curves, in: Proceedings of the 14th Int. Symp. on Industrial Crystallization, Cambridge, 12–16 September, 1999.

[15] DIN 51004, Thermal analysis (TA), Determination of melting temperatures of crystalline materials by differential thermal analysis (DTA), German Standards, 1994.
[16] M.E. Brown, Introduction to Thermal Analysis: Techniques and Applications, Chapman & Hall, London, 1988.
[17] G. Coquerel, Enantiomer 5 (2000) 481.
[18] I. Prigogine, R. Defay, Chemische Thermodynamik, VEB Deutscher Verlag für Grundstoffindustrie, Leipzig, 1962.
[19] S.G. Capewell, G.T. Hefter, P.M. May, Rev. Sci. Instrum. 70 (1999) 1481.
[20] K. Endoh, H. Suga, Thermochim. Acta 327 (1999) 133.
[21] A.S. Myerson, R. Mohan, H. Lorenz, Estimation of solubility and crystal growth kinetics using a differential scanning calorimeter, Poster Contribution 141a, in: Proceedings of the AIChE 2000 Annual Meeting, Los Angeles, 12–17 November 2000.
[22] R. Mohan, H. Lorenz, M. Rauls, A.S. Myerson, Crystal Growth & Design, 2001, in preparation.
[23] J.W. Mullin, Crystallization, Butterworth-Heinemann, Oxford, 1993.
[24] H.W.B. Roozeboom, Z. Phys. Chem. 28 (1899) 494.
[25] M. Leclercq, A. Collet, J. Jacques, Tetrahedron 32 (1976) 821.
[26] Z.J. Li, M.T. Zell, E.F. Munson, D.J.W. Grant, J. Pharm. Sci. 88 (1999) 337.
[27] W.R. Angus, R.P. Owen, J. Chem. Soc. London (1943) 227.
[28] B. Elvers (Ed.), Ullmann's Encyclopedia of Industrial Chemistry, VCH Verlagsgesellschaft mbH, Weinheim, 1989.
[29] C. Fouquey, J. Jacques, Tetrahedron 26 (1970) 5637.
[30] Beilstein's Handbuch, 4. Aufl., E I 10, Springer, Berlin, 1932.
[31] W. Holze, Thermodynamische Untersuchungen an Systemen aus optisch aktiven Weinsäure- und α-Phenylethylaminabkömmlingen, PhD thesis, Universität Magdeburg, 1967.
[32] W.R. Angus, R.P. Owen, J. Chem. Soc. London (1943) 231.
[33] N. Nishiguchi, M. Moritoki, T. Shinohara, K. Toyokura, in: G.D. Botsaris, K. Toyokura (Eds.), Separation and Purification by Crystallisation, Am. Chem. Soc., Washington, DC, 1997, p. 73.
[34] M. Rauls (BASF Ludwigshafen, Germany), Personal Information, 2000.
[35] H. Lorenz, P. Sheehan, A. Seidel-Morgenstern, J. Chromatogr. A 908 (2001) 201.
[36] W.L. McCabe, J.C. Smith, P. Harriot, Unit Operations of Chemical Engineering, International Edition, McGraw-Hill, New York, 1993.